IOP Publishing Journal of Optics
J. Opt. 17 (2015) 035901 (6pp) doi:10.1088/2040-8978/17/3/035901

Photonic quasicrystal nanopatterned silicon thin film for photovoltaic applications

H Ren[1,2], Q G Du[1,3,6], F Ren[4,5,6] and C E PNG[1]

[1] Institute of High Performance Computing, 1 Fusionopolis Way, #16-16 Connexis North, Singapore 138632
[2] Electrical Engineering, California Institute of Technology, 1200 E, California Blvd, Pasadena, CA 91125, USA
[3] Department of Physics, University of Toronto, 60 ST. George St., Toronto, Ontario, M5S 1A7, Canada
[4] Department of Electronic Materials Engineering, Research School of Physics and Engineering, The Australian National University, Canberra, ACT 0200, Australia
[5] School of Electronic Science and Engineering, Nanjing University, Nanjing 210093, People's Republic of China

E-mail: qingguodu@gmail.com and fangfang.ren@anu.edu.au

Received 7 November 2014, revised 4 January 2015
Accepted for publication 12 January 2015
Published 20 February 2015

Abstract

In this paper, the authors numerically studied the optical properties of a silicon photonic quasicrystal (PQC) nanohole array for photovoltaic applications. With the same active layer thickness, the ultimate efficiency of a solar cell integrated with an optimized PQC nanohole array can be enhanced by 9.01% and 1.40% compared to that with an ordered square lattice of a nanohole array and a random nanohole array, respectively. The absorptance enhancement is mainly due to the higher-order rotational symmetry in PQC structures, which leads to the presence of additional resonant modes, the broadening of existing modes and the reduction of surface reflectance. The angular response for both transverse-electric and transverse-magnetic modes are also analyzed in detail.

Keywords: nanostructures, photovoltaic, photonic quasicrystal

(Some figures may appear in colour only in the online journal)

Solar energy, which provided 0.7% of the world's total energy in 2013 [1], is one of the most promising renewable energies. However, the solar cell market seems to be close to saturation owing to the high price of crystalline silicon, which accounts for around 40% of the total cost of solar modules [2]. Most commercially available silicon (Si) solar cells are made of bulk Si wafers, with an active layer thickness ranging from 200 μm to 300 μm. Tremendous effort has been devoted to reducing the thickness of Si active layers to a few micrometres or even sub-micrometres in order to lower the cost of solar cell modules [3]. While a thin active layer is more efficient in charge-carrier transport, the obvious drawback is that the light absorption is weak, especially in the long wavelength range near the band edge of Si [4]. Therefore, different light-trapping techniques have been explored and employed to enhance light absorption in the active layer. For example, top and back surface texturing is intensively used for light trapping and is used in such applications as grating couplers [5, 6], randomly textured structures [7–9] and plasmonic nanostructures [10–12]. On the other hand, directly texturing an active layer into nanostructures has also been widely used to trap the light such as in nanowire structures [13–16], nanohole structures [17–20], nanocone structures [21] and nano-cone-hole structures [22]. Another strategy to introduce better light absorption is to manipulate the randomness of nanostructures to achieve additional supported guided resonant modes and to broaden existing resonant modes [20, 23–26]. Recently, quasiperiodic structures, which exhibit higher rotational symmetry, have been reported for solar cell application assisted with plasmonic effects [12] or transparent electrode patterning [27]. However, to the best of our knowledge, the light absorption enhancement using a

[6] Author to whom any correspondence should be addressed.

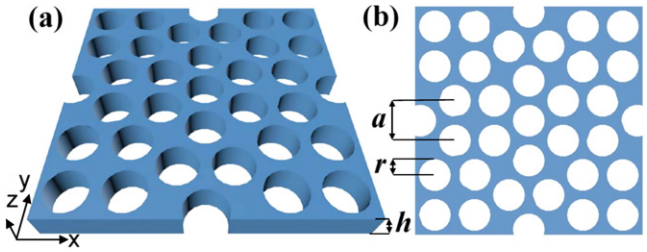

Figure 1. (a) 3D schematic and (b) 2D top view of the silicon PQC structure with a supercell simulation range.

quasiperiodically textured nanostructure in the active layer has not been studied in detail. In this paper, we propose a new type of thin film solar cells integrated with a PQC nanohole (NH) array textured crystalline silicon (c-Si) active layer. The optical properties, including absorptance, reflectance and transmittance, were numerically investigated by comparing them with other nanostructured architectures, e.g. an ordered square lattice NH array and a random NH array. For simplicity, the PQC NH array, ordered square lattice NH array and random NH array are named as PQC structures, ordered structures and random structures in the following text.

Figure 1 shows the schematic illustration of the PQC structure for the study. The three-dimensional (3D) view and two-dimensional (2D) top view of the PQC structure are shown in figures 1(a) and (b), respectively. The PQC structure has 12-fold symmetry, which is generated using the Stampfli inflation rule [28, 29]. In this method, offspring dodecagons are generated from dodecahedral parent cells with a factor of $2+\sqrt{3}$. The computing domain of $\left(4+\sqrt{3}\right)a$ is chosen in both the x and y directions in order to exhibit the long range 12-fold symmetry, suitable for simulation using the supercell theory in quasicrystal structures [30]. There are $N_q = 33$ cylinders in the simulation area; the filling factor of the PQC structure is then defined as $f_q = N_q\pi r^2/\left(4+\sqrt{3}\right)^2 a^2$ in which a is the distance between each nanohole (figure 1(b)). The thickness of the thin film is defined as h (figure 1(a)), and the radius of the NHs is indicated as r, as shown in figure 1(b). The silicon dielectric function used in our analysis is taken from [31]. For the ordered structure, a square lattice model of area a by a with one cylinder is applied for the optical property simulation; for the random structure, a randomized model of area $5a$ by $5a$ with 25 cylinders is generated for the simulation. The filling factors for ordered and random structures are $f_s = \pi r^2/a^2$ and $f_r = N_r\pi r^2/5^2a^2$, respectively, which are approximately identical to f_q. The random array used in our analysis is a general case position randomized array [25].

All the spectra simulations for PQC, ordered and random structures are calculated by employing a commercial software package (Lumerical FDTD Solutions) based on the finite-difference time-domain (FDTD) method. sunlight is perpendicularly incident on the top of the thin film. Periodic boundary conditions are used in the x and y directions, and air-Si-air layers are used in the z direction with a perfectly matched layer boundary condition adopted above and below the air layers. The reflectance (R) and transmittance (T) were calculated directly. The absorptance (A) is determined by $A = 1 - R - T$. Here, we fixed the hole distance of the PQC structure at $a = 500$ nm according to our optimization (not shown). The thickness of the c-Si film is fixed at $h = 300$ nm for all the simulations.

Figures 2(a)–(c) show the absorption, reflection and transmission spectra of the PQC, ordered and random structures when the ratio of the radius of NH (r) to lattice constant (a) $r/a = 0.4$. The results of a bare c-Si thin film without any nanostructure are also provided for reference. The spectra of the PQC structure in figures 2(a)–(c) are the average of azimuth angle $\varphi = 0°$ (angle between the E-field and x-axis) normal incident light and azimuth angle $\varphi = 90°$ normal incident light to represent unpolarized sunlight. The spectra of the random structure in figures 2(a)–(c) are the average spectra of four different randomized NH arrays, shown in the insets of figure 2(d), which were randomly generated by computer. We utilize such a physically meaningful treatment to avoid a small probability event and to represent the real situation with reference to the absorption spectra for all four cases, shown in figure 2(d). It is found that the absorption spectra of PQC, ordered and random structures almost coincide with each other in the range of short wavelengths. From $\lambda = 500$ nm onward, the PQC structure exhibits more absorption peaks, but with lower peak efficiencies, and a wider line width compared to the ordered one. It has been pointed out that the presence of the guided resonant modes in PQC and ordered structures are responsible for the existence of peaks in the absorption spectra [15, 17]. We therefore believe that the PQC structure should support additional guided resonant modes rather than the ordered structure since the former one has a higher-order rotational symmetry. It should be noted that even in the case of the random structure, the solar cells with nanostructures show higher absorption compared to the bare thin film, especially in the long wavelength range from 800 nm to 1100 nm where the absorption of the bare thin film is extremely low.

The corresponding reflectance and transmittance spectra are shown in figures 2(b) and (c). In the short wavelength range, the absorptance is mainly determined by the reflectance due to the high material absorption of Si, i.e. the lower the reflectance, the higher the absorptance. For example, the transmittance of the bare thin film is inhibited when $\lambda < 500$ nm, since the light, which has not been reflected, will be absorbed by Si. However, the thin film with nanostructures exhibits a lower reflectance compared to the bare film in this range, suggesting higher absorption efficiency, as shown in figure 2(a). In the long wavelength range where the material absorption coefficient is reduced, the absorptance will be affected by both the reflectance and the supported guided resonant modes. For instance, the reflectance of the ordered structure approaches zero at the wavelength of 970 nm (figure 2(b)), but the transmittance is quite high (figure 2(c)), which finally results in the relatively low absorption in figure 2(a). The PQC structure follows a similar behaviour as described above, despite the amplitude and position modulation of the absorption peaks.

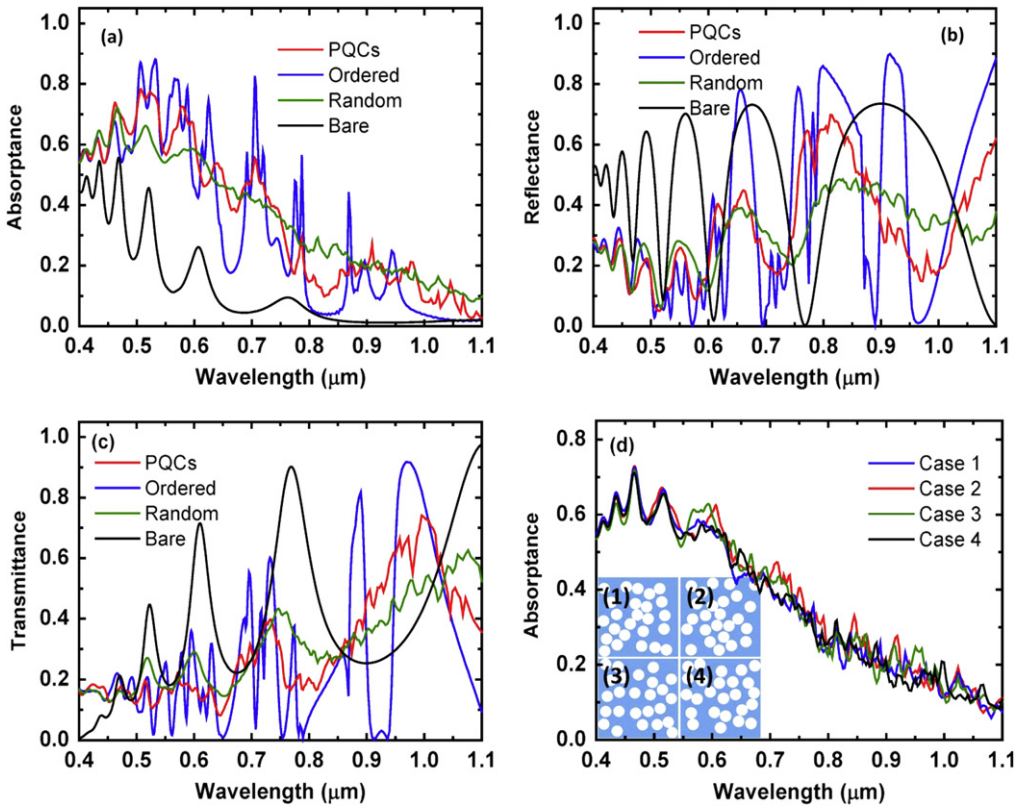

Figure 2. (a) Absorptance, (b) reflectance and (c) transmittance of PQC, ordered and random structures and (d) absorptance of four different random structures.

To further clarify the absorption properties of the nano-patterned structures, the electric- (E-) field intensity distribution for the PQC, ordered and random structures at $\lambda = 624.6$ nm and 662.4 nm are depicted in figure 3. These two wavelengths correspond to one absorption peak and to the next dip for both the PQC and ordered structures. As shown in figures 3(a) and (b), the resonant mode at 624.6 nm can be supported in both the PQC and ordered structures but with weaker confinement in the PQC case, which indicates a guided resonant mode with a lower quality factor (Q-factor) corresponding to a lower and broader peak in the absorption spectrum. Meanwhile, the field intensity in figure 3(d) is stronger than that in figure 3(e) at the wavelength of 662.4 nm due to the broadening of the guided resonant mode in the PQC structure, which agrees well with the deeper absorption dip in the ordered structure rather than the PQC case. By comparing the E-field intensity distribution in figures 3(a) and (c) or figures 3(d) and (f), we find that the PQC structure presents slightly stronger/weaker confinement at 624.6 nm/ 662 .4 nm than the random structure, which is consistent with the observation in the absorption spectra, as shown in figure 2(a). From figures 3(c) and (f), the E-field intensity distributions at these two wavelengths show similar features, which explain the flattened absorption spectrum of the random structure.

To evaluate the absorption performance of the thin film solar cell, the ultimate efficiency, η, which is defined as the efficiency of a photovoltaic cell when each photon with energy greater than the material band edge generates an electron-hole pair, needs to be calculated. η can be written as [32]

$$\eta = \frac{\int_{\lambda_{\min}}^{\lambda_g} I(\lambda) A(\lambda) \frac{\lambda}{\lambda_g} \mathrm{d}\lambda}{\int_{280\mathrm{nm}}^{4000nm} I(\lambda) \mathrm{d}\lambda} \quad (1)$$

where $I(\lambda)$ is the solar intensity per wavelength interval using the Air Mass 1.5 (AM1.5) spectrum [33], $A(\lambda)$ is the absorptance, λ is the wavelength and λ_g is the wavelength corresponding to the band edge. The ultimate efficiency of the PQC, ordered and random structures shown in figure 4(a) is calculated under normal incidence for various ratios of r/a. It is found that the efficiency from nanostructured thin film ranges from 12.23% to 17.42%, while the bare thin film only has a lower efficiency of 5.64% (indicated as the dashed line in figure 4(a)), which confirms the improvement of the light trapping and absorption. As r/a increases from 0.2 to 0.35, the efficiency of thin films with all these types of nanostructures will be increased, although the effective absorbing area is decreased. In the special range of $0.2 < r/a < 0.25$, the PQC structure is optimal among other designs due to the highest absorption. When $r/a = 0.35$, i.e. $r = 175$ nm, the efficiencies from all nanostructures reach the maximum point, which is 17.42% for the PQC structure, 1.40% higher than the random structure (17.18%) and 9.01% higher than the ordered structure (15.98%). After $r/a = 0.35$, the ultimate efficiencies of all

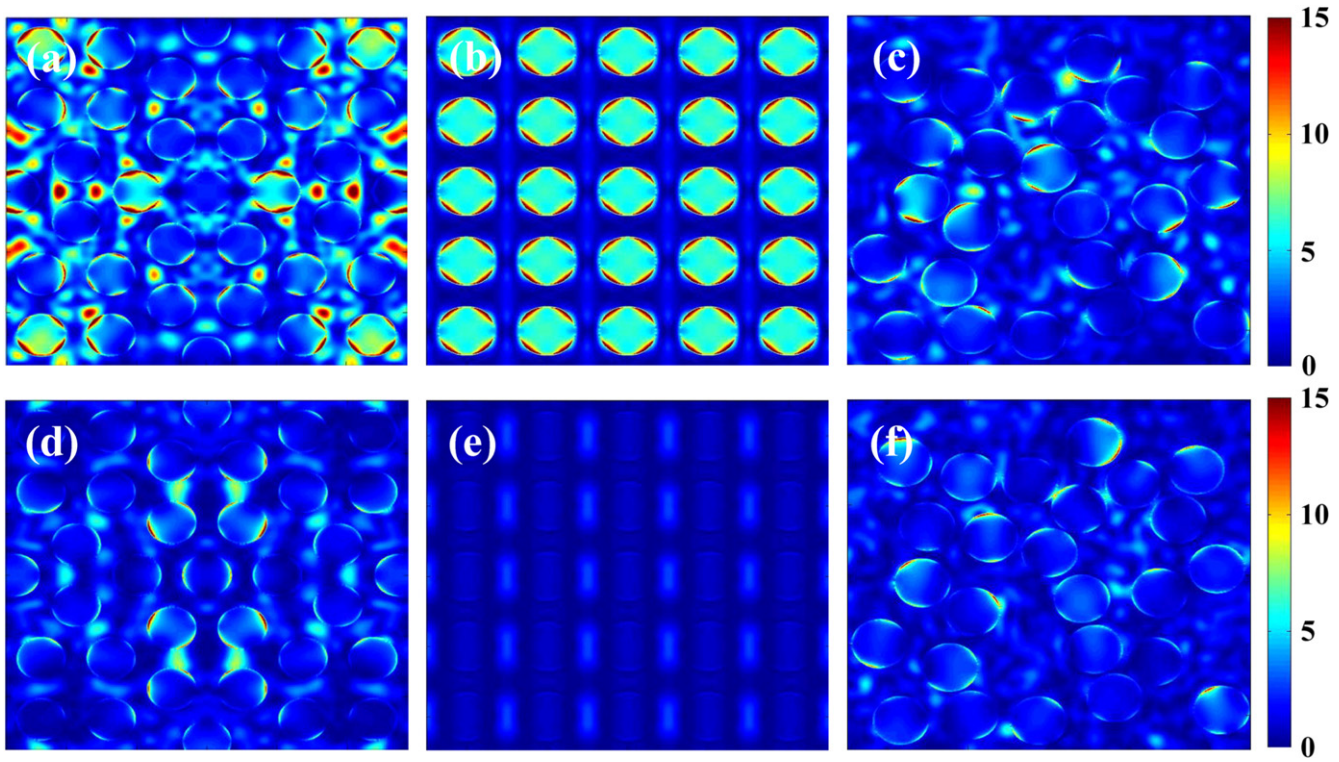

Figure 3. E-field intensity distributions (azimuth angle $\varphi = 0°$) in (a) PQC, (b) ordered and (c) random structures at $\lambda = 624.6$ nm. E-field intensity distributions in (d) PQC, (e) ordered and (f) random structures at $\lambda = 662.4$ nm.

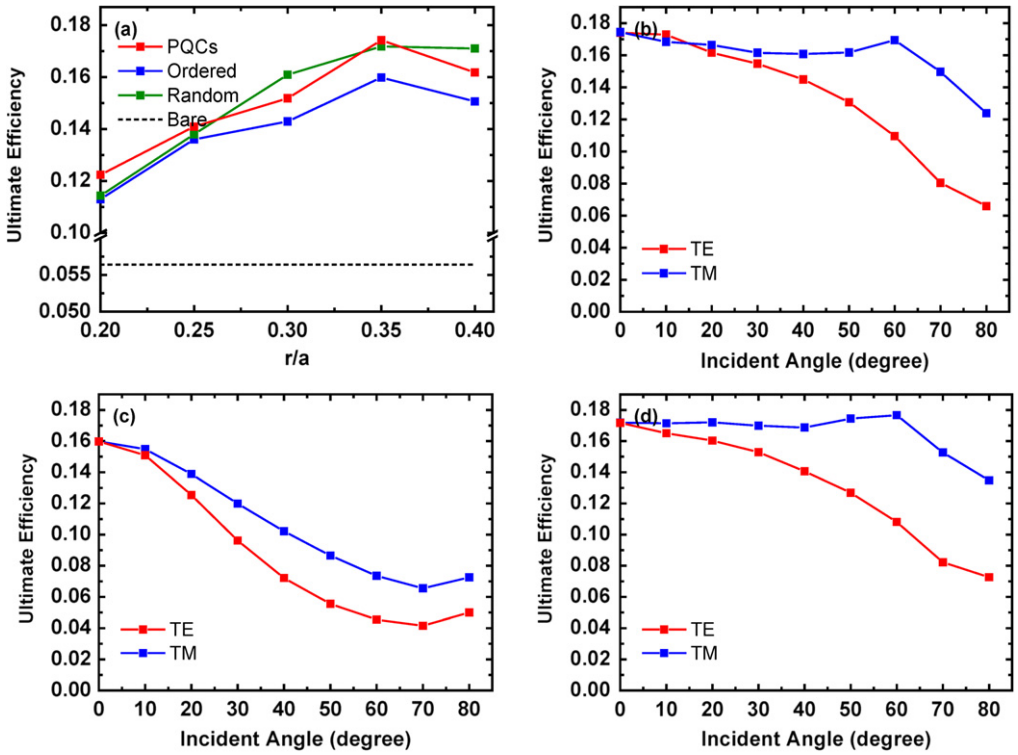

Figure 4. (a) Ultimate efficiency of the PQC, ordered and random structures for different ratios of radius of NH to lattice constant, *r*/*a*. Angular response and polarization dependence of the ultimate efficiency of the optimized (b) PQC, (c) ordered and (d) random structures.

Table 1. Ultimate efficiencies of PQC, random and ordered nanostructures with film thicknesses $h = 330$ nm (10% increased), 300 nm (original thickness) and 270 nm (10% decreased).

Film thickness h	PQC structure	random structure	ordered structure
330 nm (10% increased)	18.99%	18.30%	16.68%
300 nm (Original)	17.42%	17.18%	15.98%
270 nm (10% decreased)	15.98%	16.80%	14.30%

three structures start to decrease because of the remarkable reduction of the absorbing materials. It is also worthy to mention that the efficiency of the PQC and random structures is always larger than that of the ordered structure from $r/a = 0.2$ to 0.4, which clearly demonstrates the advantage of the PQC and random nanostructures in the photovoltaic applications.

In figures 4(b)–(d), we numerically investigated the dependence of ultimate efficiencies on the incident angles for optimized PQC, ordered and random structures under a transverse-electric (TE, no electric field in the z direction) or transverse-magnetic (TM, no magnetic field in the z direction) polarized state. It can be seen that the efficiency under TE and TM illumination drops rapidly in the ordered structure when the incident angle is increased, mainly due to the momentum mismatch between the guided modes and the incident light. However, in PQC and random structures, the efficiency of the TE polarization will be reduced more slowly, and the efficiency of the TM mode will be relatively stable with the incident angle varying from 0° up to 60°. Such a good angular response is critically important for solar energy collecting where an expensive solar tracking system is not used.

Finally, we briefly discuss the influence of the thin film thickness h on the ultimate efficiencies in PQC, ordered and random structures, which was fixed to be 300 nm in the above simulations for simplicity. By setting h to be 330, 300 and 270 nm, we performed the simulation of absorption spectra to check what the slight change of the thickness (±10%) would do. The basic parameters are set as $r/a = 0.35$ and $a = 500$ nm. The calculated ultimate efficiencies for all the nanostructures are listed in table 1. When the thickness is increased from 270 nm to 330 nm, the ultimate efficiency of each nanostructure will be improved, mainly due to the increment of absorption length. For $h = 300$ nm and 330 nm, the PQC has the best performance rather than the random and ordered structures. However, when h is decreased to 270 nm, the efficiency of the PQC is still higher than the ordered structure, but it is lower than the random structure. this indicates that the thickness of the thin film is critical for the effectiveness of the PQC structure, and one should optimize it before practical fabrication.

In conclusion, the optical properties of a 12-fold PQC nanohole array, a photonic crystal ordered square lattice of a nanohole array and a photonic crystal random nanohole array are theoretically studied for application in solar cells. It is clearly shown that a PQC structure has better absorption performance compared to ordered and random structures due to the additional supported guided resonant modes, which are introduced by higher rotational symmetry. When $r/a < 0.25$, the PQC structure is optimal among other designs. At $r/a = 0.35$, the ultimate efficiency of the PQC structure reaches the maximum value of 17.42%, which is 1.40% higher than the random structure and 9.01% higher than the ordered structure. We also studied the angle dependence of efficiency under TE and TM polarizations. The PQC and random structures exhibit higher stability against incident angle changes than the ordered structure.

This work was supported by the Australian Research Council Discovery Early Career Researcher Award (DE 130101700) and the National Natural Science Foundation of China (No. 11104130).

References

[1] www.statisticbrain.com/solar-energy-statistics/
[2] Catchpole K R and Polman A 2008 *Opt. Express* **16** 21793–800
[3] Tao M 2008 *Electrochem. Soc. Interface* **17** 30–5
[4] Redfield D 1974 *Appl. Phys. Lett.* **25** 647–8
[5] Haase C and Stiebig H 2006 *Prog. Photovolt. Res. Appl.* **14** 629–41
[6] Khan M R, Wang X, Bermel P and Alam M A 2014 *Opt. Express* **22** A973–85
[7] Yablonovitch E and Cody G D 1982 *IEEE Trans. Electron Devices* **29** 300–5
[8] Fahr S, Rockstuhl C and Lederer F 2008 *Appl. Phys. Lett.* **92** 171114–7
[9] Yu Z, Raman A and Fan S 2010 *Proc. Natl. Acad. Sci. USA* **107** 17491–6
[10] Ferry V E, Sweatlock L A, Pacifici D and Atwater H A 2008 *Nano Lett.* **8** 4391–7
[11] Atwater H A and Polman A 2010 *Nat. Mat.* **9** 205–13
[12] Bauer C and Giessen H 2013 *Opt. Express* **21** A363–71
[13] Tian B, Zheng X, Kempa T J, Fang Y, Yu N, Yu G, Huang J and Lieber C M 2007 *Nature* **449** 885–9
[14] Lin Q, Hua B, Leung S-F, Duan X and Fan Z 2013 *ACS Nano* **7** 2725–32
[15] Lin C and Povinelli M L 2009 *Opt. Express* **17** 19371–81
[16] Lin C, Huang N and Povinelli M L 2012 *Opt. Express* **20** A125–32
[17] Han S E and Chen G 2010 *Nano Lett.* **10** 1012–5
[18] Peng K-Q, Wang X, Li L, Wu X-L and Lee S-T 2010 *J. Am. Chem. Soc.* **132** 6872–3
[19] Wang F, Yu H, Li J, Sun X, Wang X and Zheng H 2010 *Opt. Lett.* **35** 40–2
[20] Lin C, Martínez L J and Povinelli M L 2013 *Opt. Express* **21** A872–82
[21] Zhu J, Yu Z, Burkhard G F, Hsu C-M, Connor S T, Xu Y, Wang Q, McGehee M, Fan S and Cui Y 2008 *Nano Lett.* **9** 279–82
[22] Du Q G, Kam C H, Demir H V, Yu H Y and Sun X W 2011 *Opt. Lett.* **36** 1713–5
[23] Ferry V E, Verschuuren M A, Lare M C V, Schropp R E I, Atwater H A and Polman A 2011 *Nano Lett.* **11** 4239–45
[24] Chutinan A and John S 2008 *Phys. Rev.* A **78** 023825
[25] Du Q G, Kam C H, Demir H V, Yu H Y and Sun X W 2011 *Opt. Lett.* **36** 1884–6
[26] Bao H and Ruan X 2010 *Opt. Lett.* **35** 3378–80

[27] Tseng P C, Hsu M H, Tsai M A, Chu C W, Kuo H C and Yu P 2011 *Org. Electron.* **12** 886–90
[28] Zoorob M E, Charlton M D B, Parker G J, Baumberg J J and Netti M C 2000 *Nature* **404** 740–3
[29] Oxborrow M and Henley C L 1993 *Phys. Rev.* B **48** 6966–98
[30] Villa A D, Enoch S, Tayeb G, Poerro V, Galdi V and Capolino F 2005 *Phys. Rev. Lett.* **94** 183903
[31] Palik E D 1998 *Handbook of Optical Constants of Solids* (Boston, MA: Academic Press)
[32] Shockley W and Queisser H J 2004 *J. Appl. Phys.* **32** 510–9
[33] http://rredc.nrel.gov/solar/spectra/am1.5/